arthropoda

MDPI

Article

A New Species of *Mastigoproctus* Pocock, 1894 (Arachnida: Thelyphonida), from Jalisco, Mexico †

Carlos A. Torres-Muñoz, André F. A. Lira and Edmundo González-Santillán *

Colección Nacional de Arácnidos, Instituto de Biología, Universidad Nacional Autónoma de México, Ciudad Universitaria, Coyoacán, Ciudad de México 04510, Mexico; carlostm.17@hotmail.com (C.A.T.-M.); andref.lira@gmail.com (A.F.A.L.)

* Correspondence: edmundo.gonzalez@ib.unam.mx

† Urn:lsid:zoobank.org:act:D298B8CB-DF70-47EC-824E-F996C8074428.

Abstract

In this contribution, we describe a new species from the Estación de Biología Chamela (IBUNAM), located in Jalisco, Mexico. *Mastigoproctus claritae* sp. nov. has a stridulatory organ like *M. mexicanus* and *M. xetame.* However, it is distinguished from these species by the presence of a proventral marginal smooth keel in the chelicerae, a retrolateral surface pedipalp femur with congregated and blunt cristulae, a prodorsal margin spine S3 that is longer than the other spines in males, and symmetric, peanut-shaped spermatheca seminal receptacles in females. *Mastigoproctus claritae* sp. nov. represents the twenty-third species of the genus and the twelfth species documented in Mexico.

Keywords: whip scorpion; Linnean shortfall; taxonomy

1. Introduction

Several studies, e.g., Refs. [1–3], have indicated that biodiversity is facing a crisis, with extinction occurring at accelerated rates compared to the prior five mass extinctions. This is particularly concerning given that our understanding of biodiversity is hampered by the Linnean shortfall [4,5]. This shortfall refers to the gap in taxonomic knowledge, which is the difference between the number of species described and the actual number of species that exist in nature [5]. This concept is crucial for biodiversity conservation purposes, as it highlights the incompleteness of taxonomic records and the ongoing need for exploration and description of new species [6,7]. Consequently, it represents one of the major challenges in conservation biology, as it prevents a precise understanding of global biodiversity and hinders the development of effective strategies for protecting species and ecosystems [7].

The smaller arachnid orders (e.g., Thelyphonida, Pseudoscorpiones, and Ricinulei) are frequently underrepresented in taxonomic studies, a phenomenon that can be attributed to their comparatively lower diversity when contrasted with more abundant groups such as Araneae [8,9]. These three orders together encompass 3686 extant species, a figure that stands in stark contrast to the 53,915 species of spiders [10,11]. Despite their comparatively limited richness, these arachnids fulfill pivotal ecological functions as predators, regulating populations of insects and other invertebrates within their respective ecosystems [12]. However, the paucity of detailed studies on these groups has resulted in a gap in taxonomic knowledge, which can hinder conservation and environmental management efforts [13].

Among the small arachnid orders, Thelyphonida, commonly known as whip scorpions or vinegaroons, comprise 128 extant species distributed worldwide [14]. Notably, the

Check for updates

Academic Editor: Matthew R. Graham

Received: 11 February 2026
Revised: 27 May 2026
Accepted: 10 June 2026
Published: 13 June 2026

Copyright: © 2026 by the authors. Licensee MDPI, Basel, Switzerland. This article is an open access article distributed under the terms and conditions of the Creative Commons Attribution (CC BY) license.

thelyphonid genus *Mastigoproctus* Pocock, 1894, which is distributed from the southern United States to northern South America [15], has recently attracted researchers' attention with the description of several new species. For example, in Mexico, since 2018, seven new *Mastigoproctus* species have been described [15–17], thereby elevating the country to having the highest number of species, with over 10 described species. However, Ref. [15] indicated the existence of several undescribed species still present in the country. Therefore, with the aim of mitigating the Linnean shortfall, we describe a new species of thelyphonid belonging to the *Mastigoproctus* genus from Mexico.

2. Materials and Methods

Specimens were collected during the nighttime manually. The material examined is deposited in the Colección Nacional de Arácnidos (CNAN) and the Estación de Biología Chamela collection, Instituto de Biología, Universidad Nacional Autónoma de México (IBUNAM).

Chelicerae, pedipalps, and genitalia were dissected using forceps, scissors, and needles. Soft tissue was removed using needles to expose hardened or sclerotized structures.

Measurements and morphological terminology follow Refs. [15,16]; for the pedipalp segments, they follow Refs. [17,18]; for spination pedipalp trochanter, female genitalia, and cuticular ornamentation, they follow Ref. [15]; for carapace terminology, they follow Ref. [19]; and for male genitalia, they follow Ref. [20]. Given the absence of standardized measurements and the unavailability of standardized landmarks, the holotype of *Mastigoproctus xetame* Barrales-Alcalá & Francke, 2023 (CNAN-T1502) was used to ascertain the landmarks utilized by the authors and to compare them with our own.

Photography and measurements (in millimeters) were conducted using the Raising View software Version X64, 4.1122070.20230204 with an E3ISPM20000KPA Sony Digital Camera (ToupTek Photonics, Hangzhou, China) attached to a ZEISS SteREO Discovery.V8 stereomicroscope (Carl Zeiss AG, Jena, Germany). The total length was measured using a digital caliper. Habitus images in dorsal and ventral aspects were captured using a Sony a6400 camera (Sony Corporation, Bangkok, Thailand) equipped with a Laowa 100 mm f/2.8 2:1 Ultra Macro APO lens. The image was subjected to a series of modifications and adjustments using Adobe Photoshop CS2 and CS5. These modifications encompassed the editing of the image and the preparation of the plates. Photographic documentation of *M. xetame* and *M. mexicanus* is presented for the purpose of comparative analysis.

A map depicting the updated distribution of the genus *Mastigoproctus* spp. in Mexico was produced using QGIS version 3.26.3-Buenos Aires (https://qgis.org/, accessed on 14 January 2024). The political boundaries of the Mexican states were obtained from the CONABIO portal. (http://geoportal.conabio.gob.mx/metadatos/doc/html/dest2019gw.html, accessed on 7 July 2025). The elevation model was constructed using data from http://srtm.csi.cgiar.org (accessed on 20 February 2025).

3. Taxonomy

Family Thelyphonidae Lucas, 1835;

Subfamily Mastigoproctinae Speijer, 1933;

Genus *Mastigoproctus* Pocock, 1894;

Mastigoproctus claritae, sp. nov.

Figures 1–17, Tables 1 and 2.

Etymology. The species epithet *claritae* sp. nov. is derived from the diminutive form of Clara and serves to honor Clara Muñoz Ramírez, the mother of the first author.

Type material

Holotype

- One ♂(CNAN-T01880), MÉXICO, Jalisco, Municipio La Huerta, Estación de Biología Chamela, IBUNAM. 19°29′54″ N, 105°02′40″ W, 91 m, viii.2024, A.F.A. Lira, L.S. Rodríguez-Medina.

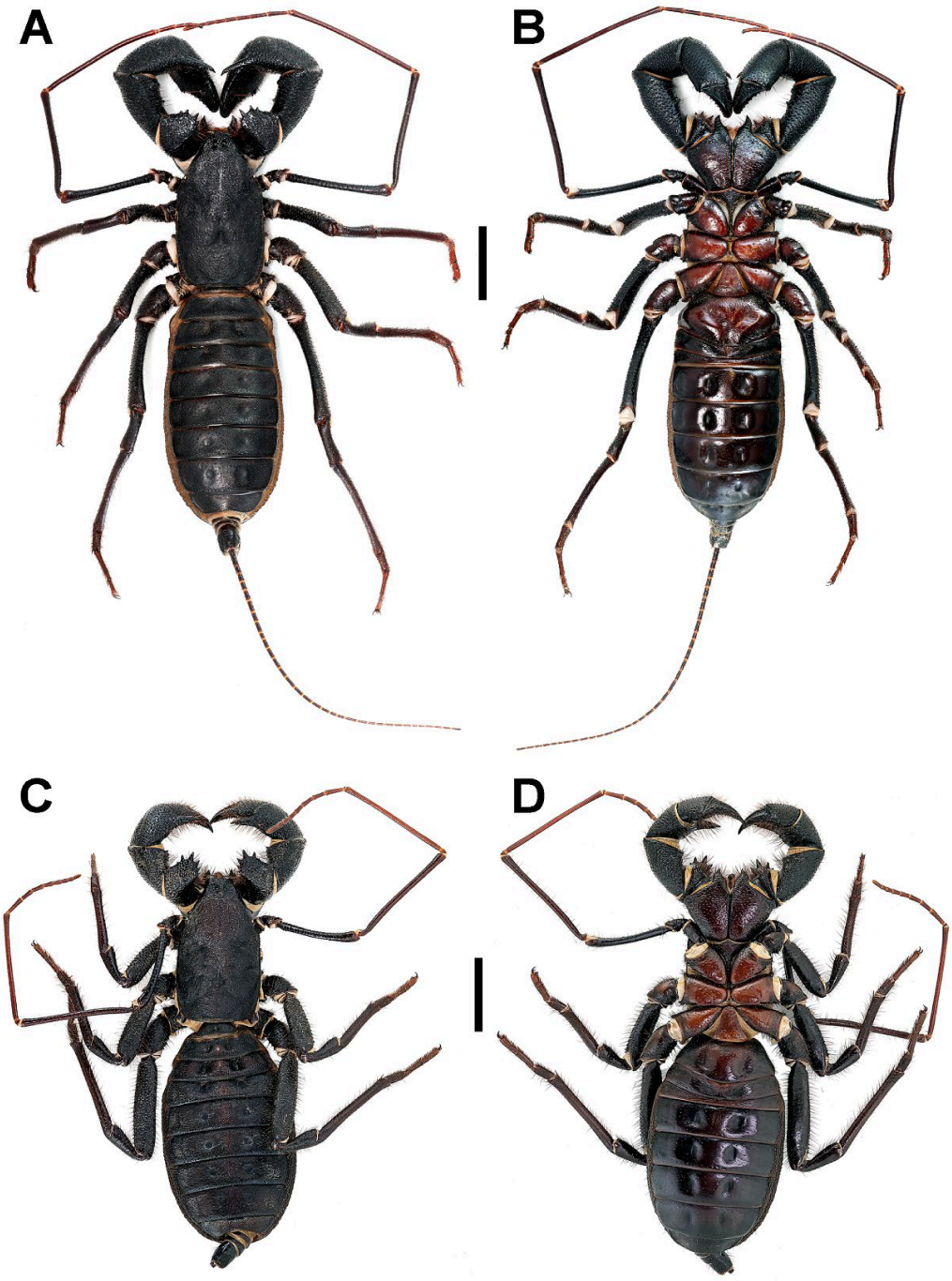

Figure 1. *Mastigoproctus claritae* sp. nov. Habitus. Dorsal (**A**,**C**) and ventral (**B**,**D**) view. Holotype ♂(CNAN-T1880) (**A**,**B**), Paratype ♀(CNAN-T01884) (**C**,**D**). Scale bar = 10 mm.

Paratypes

- One ♂, same locality, 18.vii. 2024. G. Montiel-Parra (CNAN-T01881). ● One ♂, viii.2024, A.F.A. Lira, L.S. Rodríguez-Medina (CNAN-T01882). ● One ♂, Cerro Careyes (probably Pueblo Careyes), 19°26′37″ N, 105°01′23″ W, 16 m, B. Miller (CNAN-T01883). ● One ♀, 10.viii.2016 (CNAN-T01884). ● One ♀, 15.x.1994, A.B. López L. (CNAN-T01885).

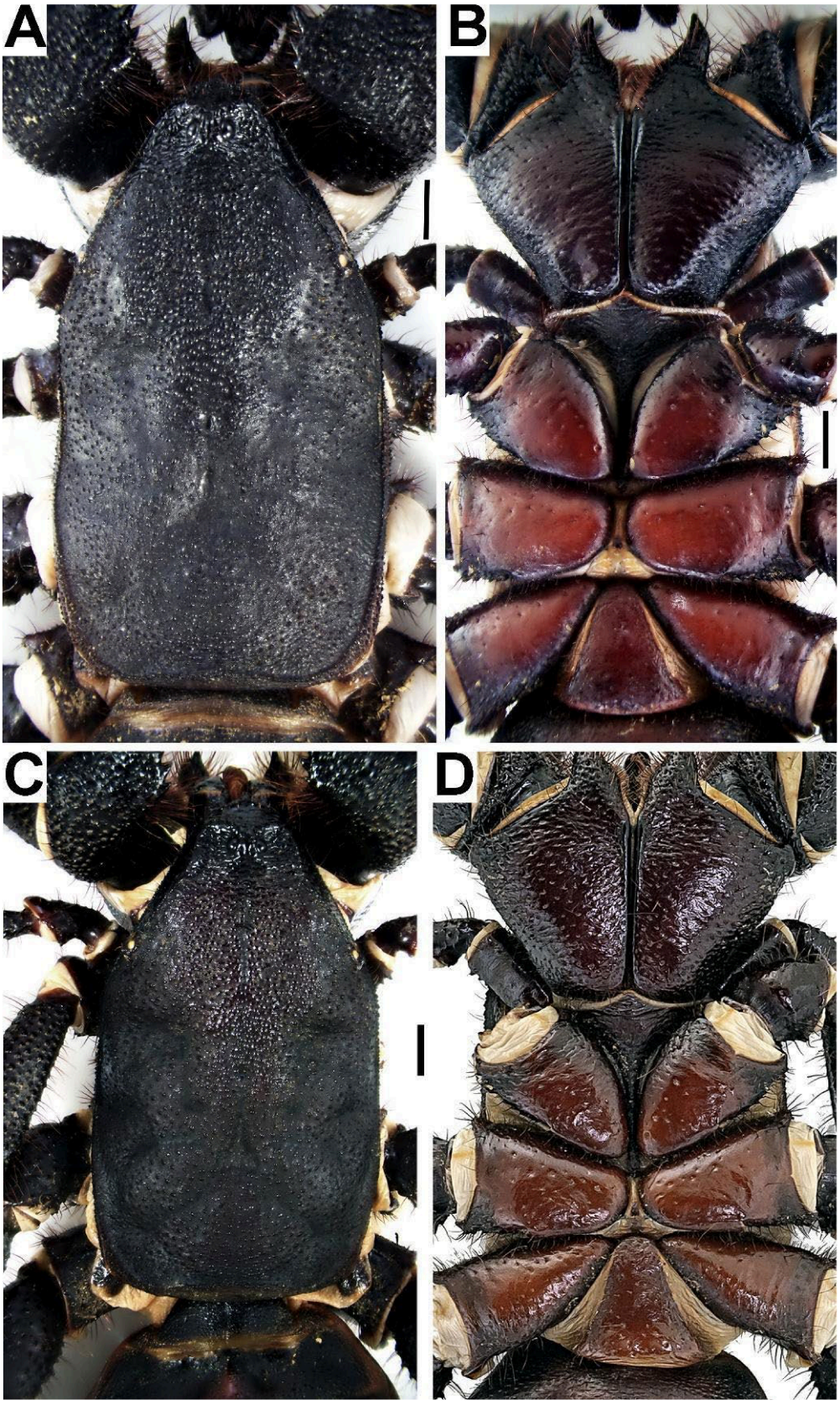

Figure 2. *Mastigoproctus claritae* sp. nov. Dorsal (**A**,**C**) and ventral (**B**,**D**) view of prosoma. Holotype ♂(CNAN-T01880) (**A**,**B**), Paratype ♀(CNAN-T01884) (**C**,**D**). Scale bar = 2 mm.

https://doi.org/10.3390/arthropoda4020009

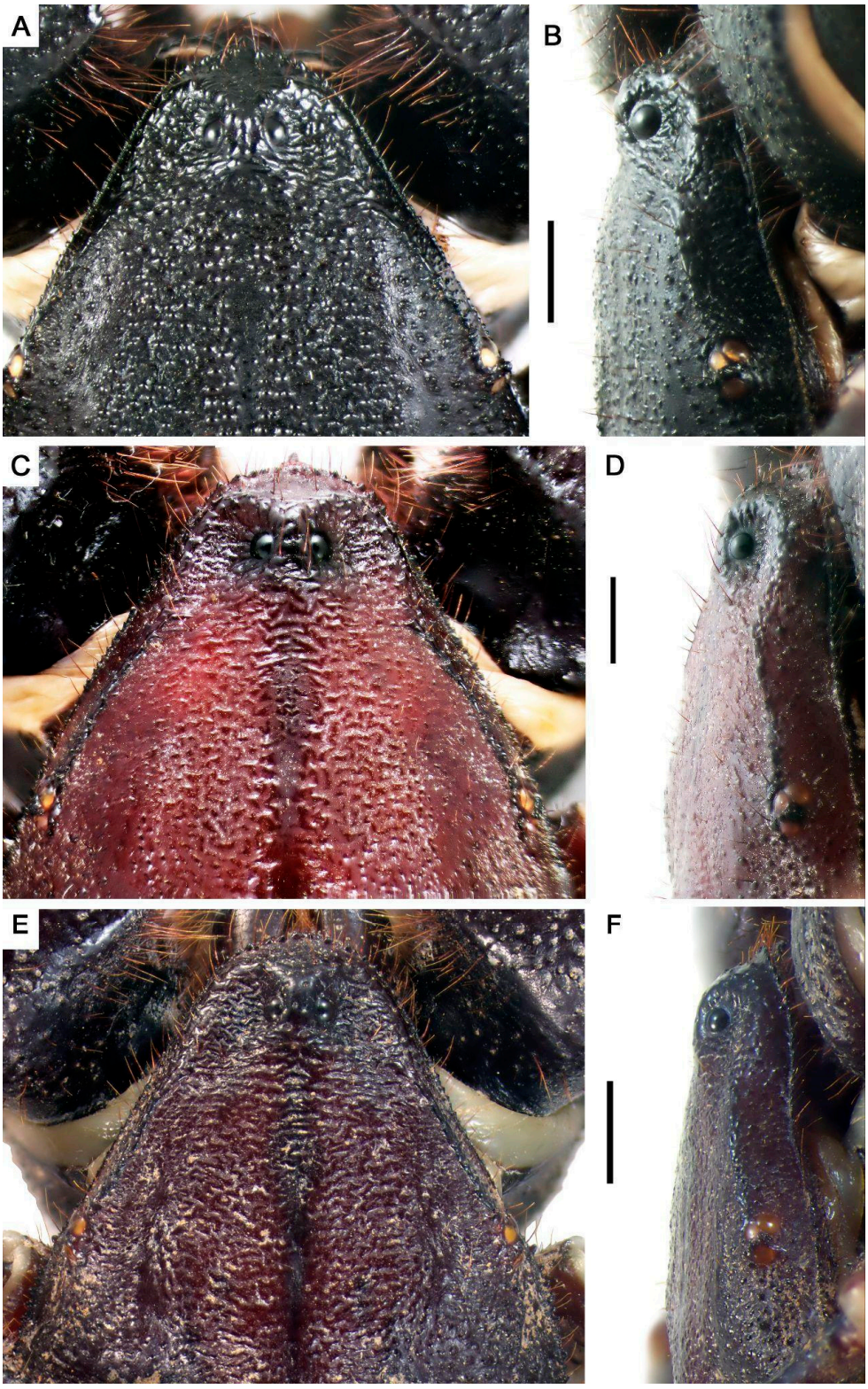

Figure 3. *Mastigoproctus* median ocular tubercle. Anterior surface (**A**,**C**,**E**) and lateral (**B**,**D**,**F**) view. *Mastigoproctus claritae* sp. nov. (**A**,**B**) Holotype ♂(CNAN-T1880). *Mastigoproctus xetame* (**C**,**D**) Holotype ♂(CNAN-T1502), *Mastigoproctus mexicanus* ♂(**E**,**F**) (CNAN-Ur0127). Scale bar = 2 mm.

Additional material examined

Mastigoproctus xetame

- (CNAN-T01502) Holotype ♂MEXICO, Jalisco, Municipio Zapopan, Bosque de la Primavera, 20°41′19.8168″ N, 103°36′32.6304″ W, 1649 m, 18.ix.2020, D. Barrales, G. Contreras, mixed pine/oak forest. ● Paratype ♀, same locality (CNAN-T01504).
- One ♂, Municipio Mazamitla, Sierra Vista Adventure, Rd. Mazamitla-Tamazula Km 5, 19°53′54.8268″ N, 103°3′48.0276″ W, 2067 m, 25.viii.2017, J. Mendoza, R. Ramírez, Loc 27, daytime collection, pine–oak forest (CNAN-UR0126).

Mastigoproctus mexicanus

One ♂, three ♀, MEXICO, Durango, Rancho La Peña, 20 km SE of Durango [23°44′0.166″ N, 104°29′52.276″ W], 2418 m, 4.v.1977, López Vidal J.C., pine–oak forest mixed with grassland, under rocks (CNAN-Ur0127). ● One ♂, Municipio San Dimas, 6.5 km south of Tayoltita, 24°3.94′ N, 105° 53.15′ W, 1004 m, 12.viii.2008. (CNAN-Ur0058) ● One ♀, Zacatecas, El Mirador, Sierra del Valparaiso, Municipio Valparaiso [22°43′21.61″ N, 103°27′23.57″ W, 2198 m, 21.ix.2001], M. Espino, R. Martínez, D. García, E. González, oak forest (CNAN-Ur0014).

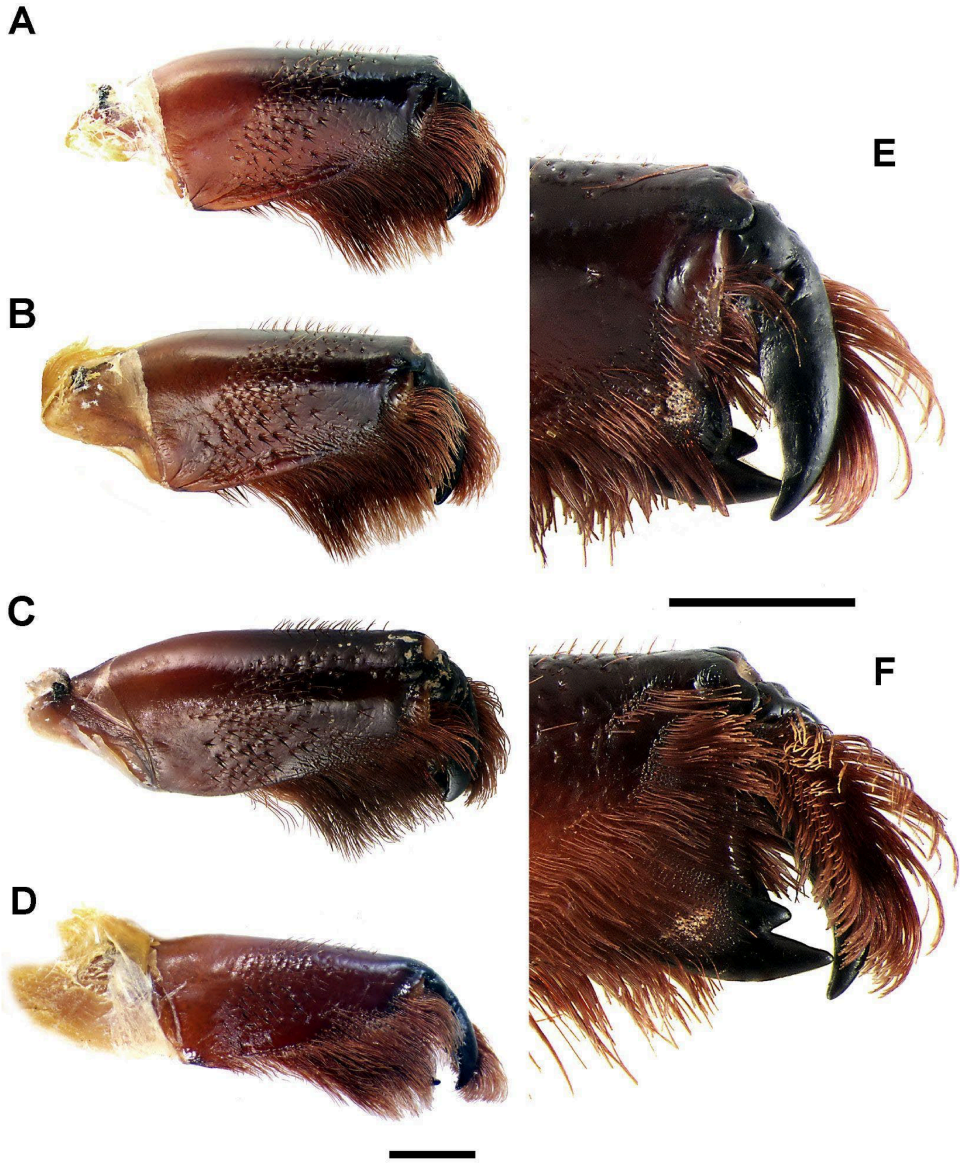

Figure 4. *Mastigoproctus* dextral chelicerae and cheliceral teeth. Retrolateral (**A**,**B**,**C**,**D**,**E**) and prolateral (**F**) view. *Mastigoproctus claritae* sp. nov. Paratype ♂(CNAN-T1881) (**A**,**E**,**F**), Paratype ♀(CNAN-T1884) (**B**). *Mastigoproctus xetame* ♂(CNAN-Ur0126) (**C**), *Mastigoproctus mexicanus* ♂(CNAN-Ur0058) (**D**). Scale bar 2 = mm.

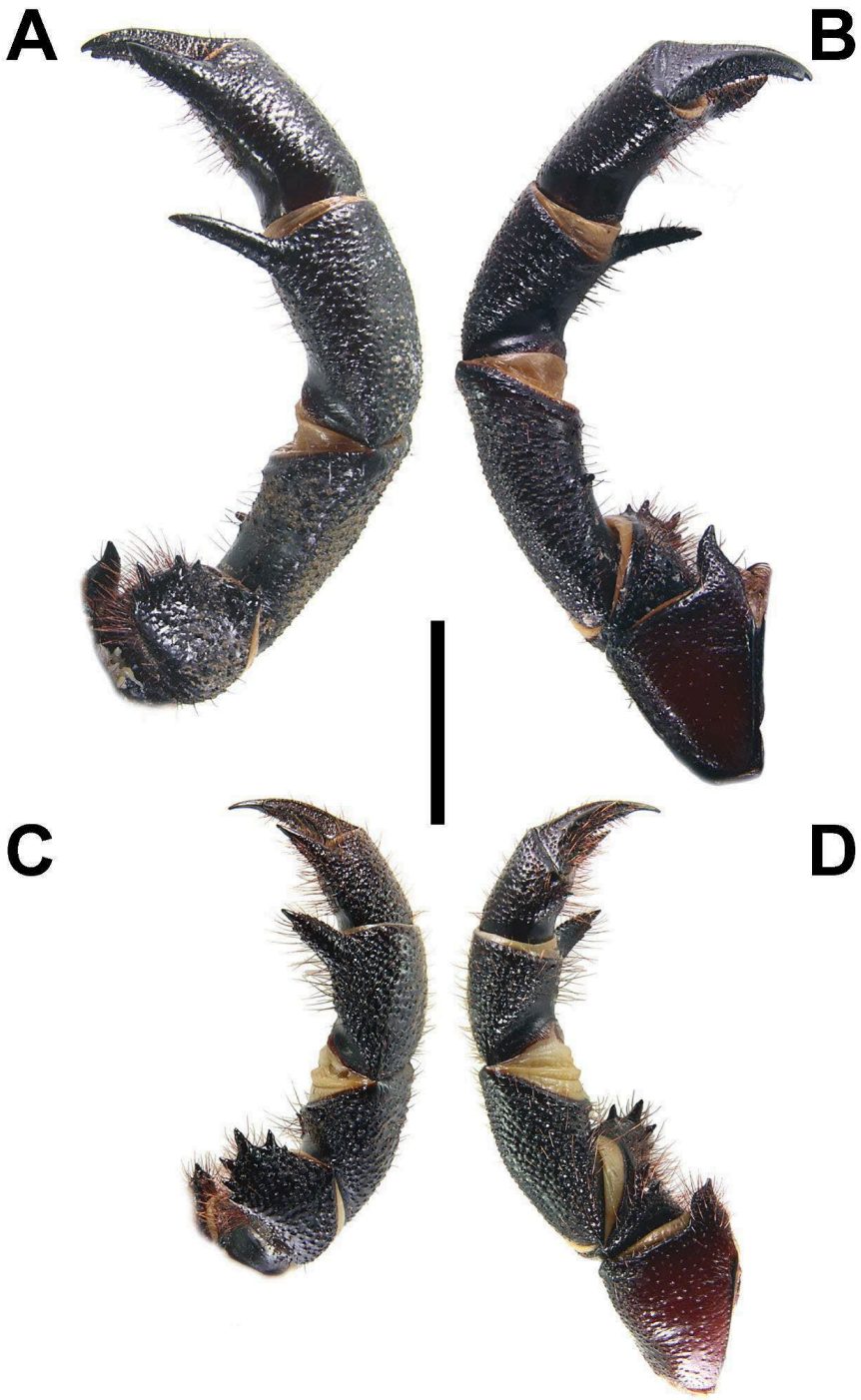

Figure 5. *Mastigoproctus claritae* sp. nov. Dextral pedipalp. Dorsal (**A**,**C**) and ventral (**B**,**D**) view. Holotype ♂(CNAN-T1880) (**A**,**B**), Paratype ♀(CNAN-T1884) (**C**,**D**). Scale bar 10 mm.

Diagnosis. *Mastigoproctus claritae* sp. nov. resembles *M. xetame* and *Mastigoproctus mexicanus* Butler, 1872. In these species, both sexes are equipped with a stridulatory organ comprising setae and cristulae on the retrolateral surface of the chelicerae and the retroventral surface of the coxae. However, *M. claritae* sp. nov. can be separated from these species by the presence of a smooth keel in the proventral margin of the chelicerae, which is absent in *M. xetame* and *M. mexicanus*. The median ocular tubercle in *M. xetame* and *M. mexicanus* is low and smooth, whereas in *M. claritae* sp. nov., it is elevated and crenulated. The body color in *M. mexicanus* and *M. xetame* is reddish to dark reddish brown, whereas in *M. claritae* sp. nov., the color is mainly brownish to mahogany. The retrolateral surface of

the pedipalp femur in these species presents several differences in ornamentation. Males of *Mastigoproctus mexicanus* present long, straight, and digitiform tubercles, whereas *M. xetame* and *M. claritae* sp. nov. present cristulae. In *M. xetame*, the cristulae are scattered and conical, whereas in *M. claritae*, the cristulae are congregated and blunt. In *M. xetame*, the spine S4 on the prodorsal margin of the pedipalp trochanter is longer than the other spines, whereas in *M. claritae* sp. nov., the spine S3 is longer than the others. *M. mexianus* exhibits S4 and S5 of equal length, whereas in *M. claritae* sp. nv., S4 is longer than S5. In females, the shape of spermathecal receptacles also differs in these species. In the lateral view, the spermathecal receptacles of *M. mexicanus* are swollen, obovate, and anteriorly directed, whereas in *M. xetame* and *M. claritae* sp. nov., they are rounded and posteriorly directed. Furthermore, in *M. claritae* sp. nov., the spermathecal receptacles are peanut-shaped and symmetric.

Description. The following description is based on the holotype male and three male and two female paratypes.

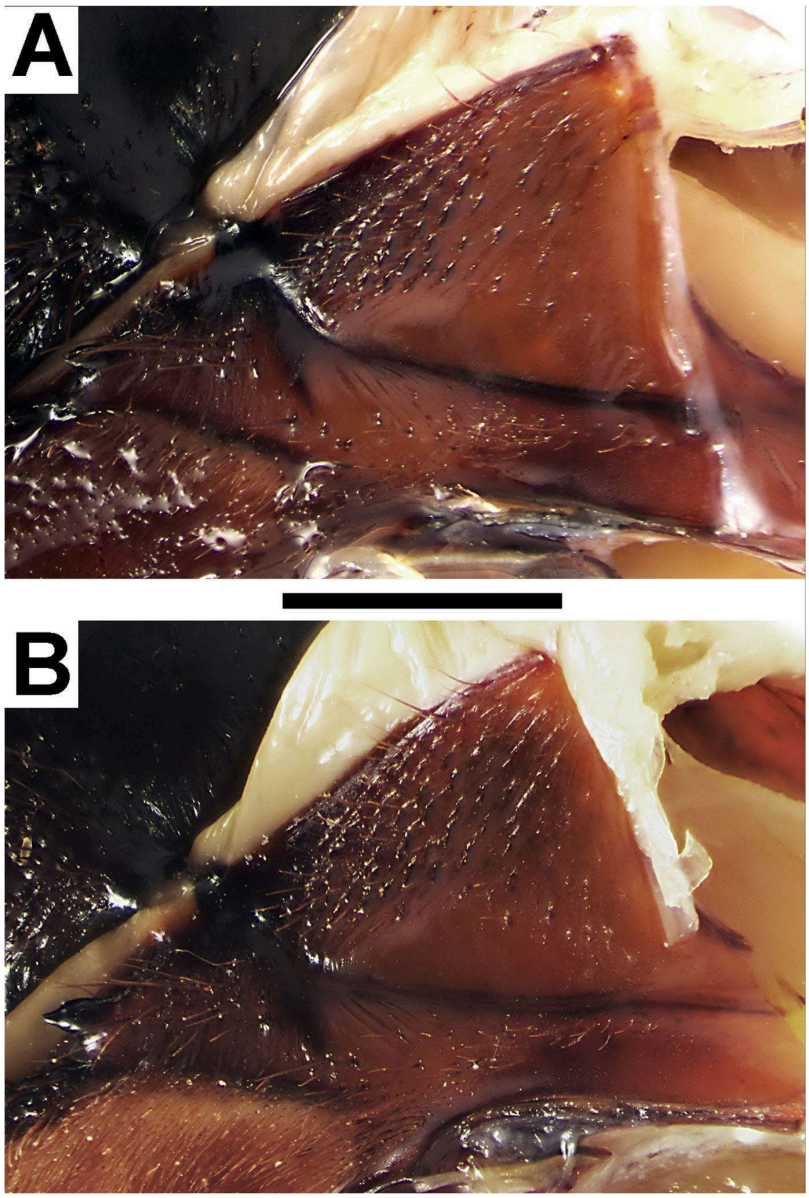

Figure 6. *Mastigoproctus claritae* sp. nov. Dextral pedipalp coxae, dorsomedial aspect. Paratype ♂(CNAN-T1881) (**A**), Paratype ♀(CNAN-T1884) (**B**). Scale bar = 2 mm.

Total length: Maximum length from anterior margin of carapace to posterior margin of opisthosomal segment XII (pygidium) in adult specimens 56.2 mm (male) and 52.1 mm (female) (Table 1).

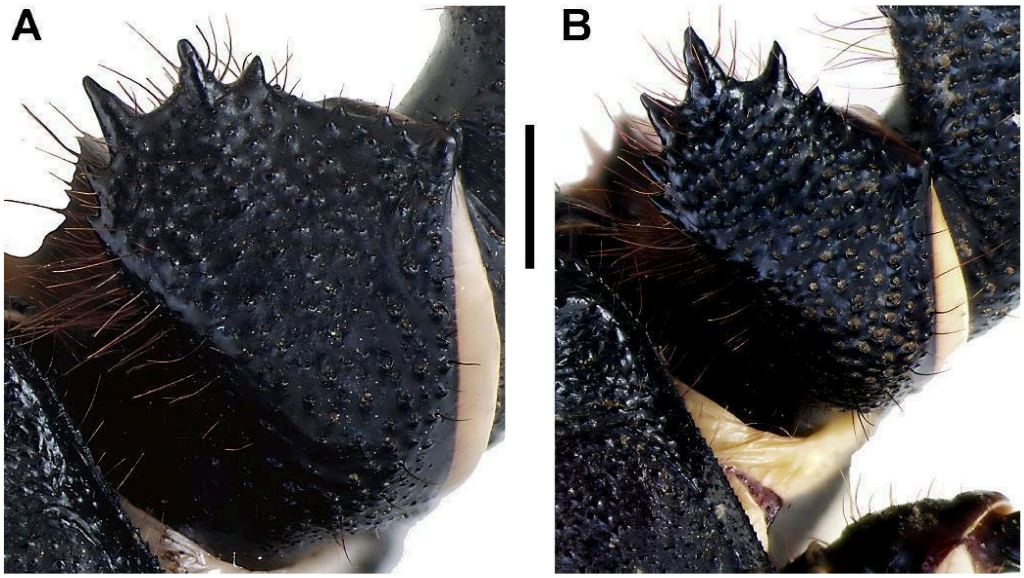

Figure 7. *Mastigoproctus claritae* sp. nov. Dextral pedipalp trochanter. Dorsal view. Holotype ♂(CNAN-T1880) (**A**), Paratype ♀(CNAN-T1884) (**B**). Scale bar = 2 mm.

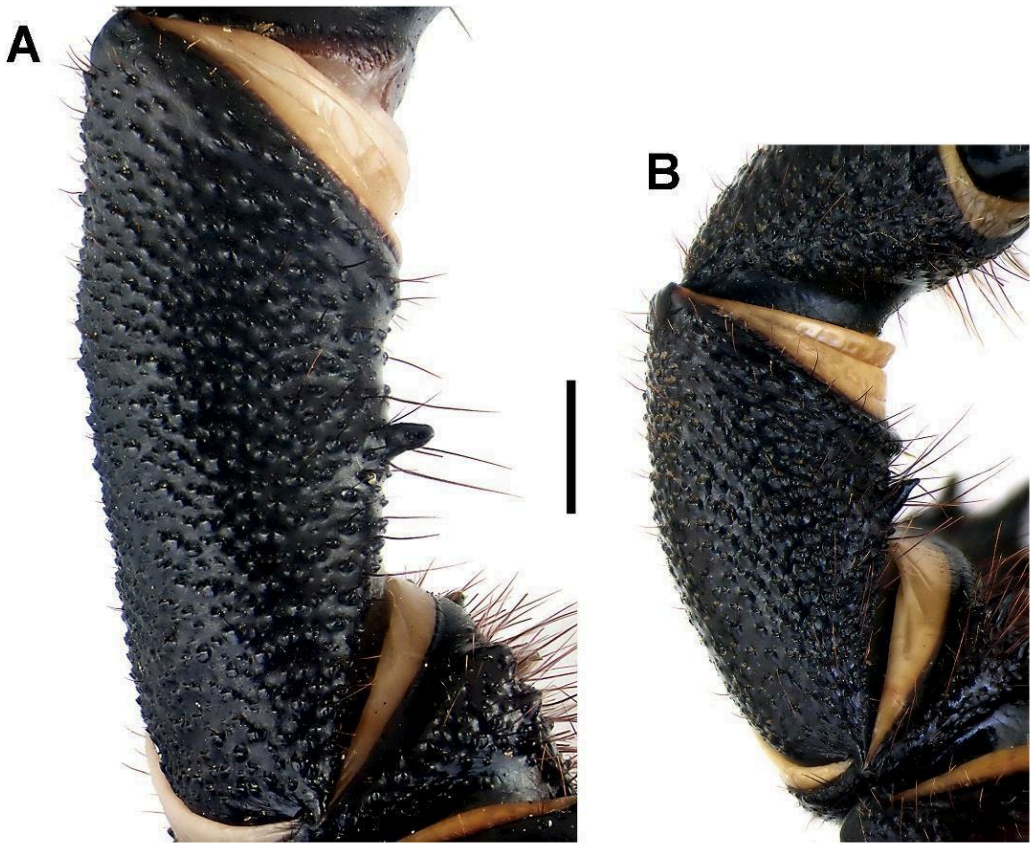

Figure 8. *Mastigoproctus claritae* sp. nov. Femur ventral view, proventral spine. Holotype ♂(CNAN-T1880) (**A**), Paratype ♀(CNAN-T1884) (**B**). Scale bar = 2 mm.

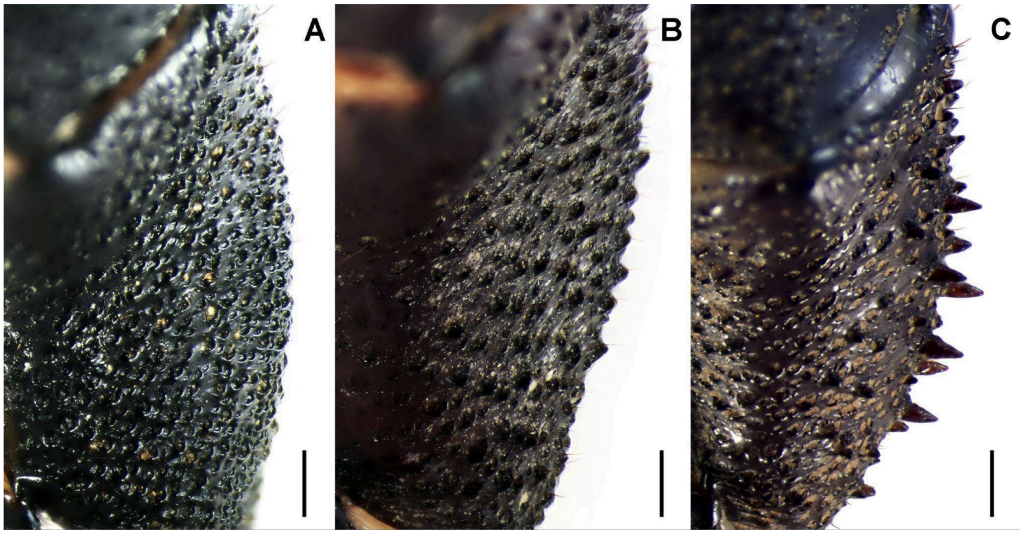

Figure 9. *Mastigoproctus* spp. Femur retrolateral view ornamentation. *Mastigoproctus claritae* sp. nov. Holotype ♂(CNAN-T1880) (**A**). *Mastigoproctus xetame* Holotype ♂(CNAN-T1502) (**B**), *Mastigoproctus mexicanus* ♂(CNAN-Ur0127) (**C**). Scale bar = 1 mm.

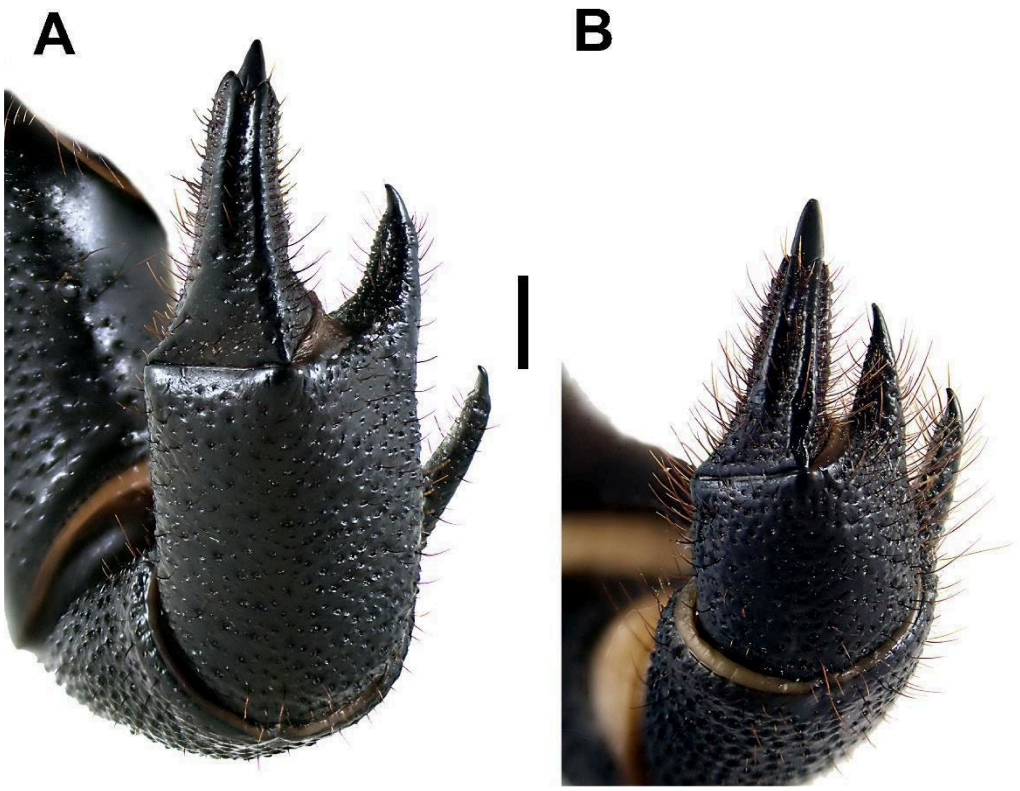

Figure 10. *Mastigoproctus claritae* sp. nov. Pedipalp tibiae and tarsi. Retrolateral view. Holotype ♂(CNAN-T1880) (**A**), Paratype ♀(CNAN-T1884) (**B**). Scale bar = 2 mm.

Coloration (Figure 1): Carapace surface brownish to mahogany more so around fovea with margins comparatively darker, median ocular tubercle darker than margins. Prosternum, mesosternum dark brown, and metasternum reddish. Chelicerae movable finger blackish, fixed finger distal area brownish, proximal area orangish. Pedipalp coxa mahogany ventral surface and dorsal-medial surface orangish. Trochanter, femur, patella and tibia, dark brownish, prolateral surface with several dark reddish macrosetae. Legs coxae I brownish, II–IV ventral surfaces orangish. Trochanter, femur and patella brownish, tarsi orangish. Tergites I–IX homogeneously mahogany, except for tergite I lighter reddish.

Sternite I anterior area orangish brown, turning yellowish to the posterior margin, sternites II–VIII mahogany, except for sternite II with shades of yellowish on the anterior margin, sternite IX dark brownish, and pygidium X and XI slightly less dark brownish dorsal area and darker on the ventral area, sternite XII homogeneously dark brown. Ommatoids are orange opaque. Flagellum is dark brown. Flagellar organs are beige yellowish.



Figure 11. *Mastigoproctus claritae* sp. nov. Legs. Legs II (**A**), III (**B**) and IV (**C**) in ventral view. Leg 1 (**D**) in lateral view. Holotype ♂(CNAN-T1880). Arrow indicates a trichobotrium. Scale bar = 2 mm.

Carapace: Surface granular with serrate margin (Figure 2). Epistome visible in the dorsal surface. Median ocular tubercle crenulate, situated near the anterior margin of carapace; surrounded by weak crests creating shallow eye sockets and visible raised (Figure 3). Anterolateral margin with a pair of strongly developed carinae anterolaterally, extending from lateral ocelli to two-thirds the distance to median ocular tubercle (Figure 3B). Distance between ocelli twice to ocular diameter. Three pairs of lateral ocelli, anterior ocelli twice the size of posterior two ocelli, which are equal size (Figure 3A,B); anterior and median ocelli separated from posterior ocellus pair by a tubercle; distance between median and posterior ocelli 9× the distance between anterior and median ocelli. Posterior fovea present, distinct.

Coxosternal region: Pedipalp coxae larger than leg coxae surface relatively smooth with small and scatter cristulae (male) or densely cristulae (female). First coxa (antenniform) slender than coxae II–IV (Figure 2A,B). Anterior sternum plaque medially broad, laterally tapered, anterior margin with a short median projection; posterior margin elongated, tapered, and deepening between first pair of coxae (Figure 2B,D). Coxa II–IV polygonal to conical with surface mostly lustrous and smooth. Posterior sternum triangular, truncated (Figure 2B,D).

Chelicerae: Manus retrolateral anterior margin with long red brownish macrosetae; prolateral with the same setose area and with about one sixth of anterior surface covered

with similar macrosetae but shorter (Figure 4); dorsal base of manus with an irregular, blackish tubercle; retrolateral surface with a stridulatory plectrum, comprising more than 25 long spines with a wide base tapering at the apex, each setae directed anteroventrally; subventral margin smooth with and evident smooth keel on proximal two thirds (Figure 4A,B). Fixed finger bears a blunt, wide, submedian, retrolateral tooth in line with a conical, prolateral tooth (Figure 4E,F). Movable finger toothless, curved with a tuft of long red brownish macrosetae on the prolateral surface, except for the apical area.

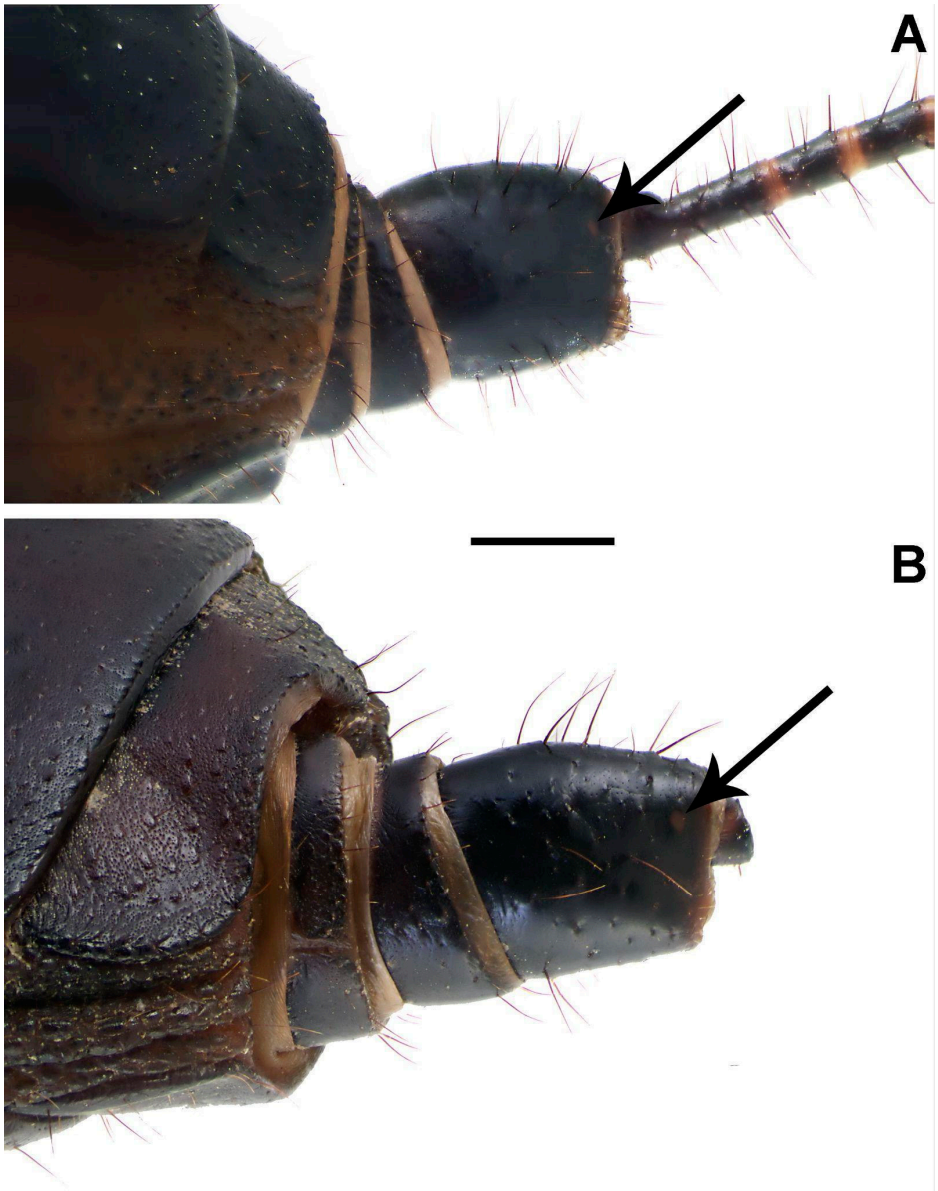

Figure 12. *Mastigoproctus claritae* sp. nov. Pygidium and flagellum. Lateral view. Holotype ♂(CNAN-T1880) (**A**,**B**), Paratype ♀(CNAN-T1884). Arrows indicate ovate ommatoids. Scale bar = 2 mm.

Pedipalps: Dorsal, ventral, and retrolateral cuticular surfaces densely covered with cristulae, less developed distally from coxa to tibia, prolateral surface mostly smooth with red setae (Figure 5). Coxa, retrolateral surface with reduced cristulae; ventral surface rugose; coxal apophysis with a row of progressively larger spines on prodorsal margin and with a terminal larger spine; prodorsal posterior half surface with long, retroventrally directed macrosetae inserted in cristulae, forming stridulatory surface (pars stridens) (Figure 6); prodorsal anterior half surface, part of the oral apparatus, with abundant short setae.

Trochanter longer than wide (male), or subquadrangular (female); retrodorsal surface with dense cristulae (male) or reduced cristulae (female) (Figures 5 and 7); prodorsal margin with five terminal spines (S1–S5) and one subterminal accessory spine (AS) on prolateral surface present (females) or absent (males), spines size variation S3 > S4 > S2 ≥ S5 > S1 (Figure 7A) (male) or S4 > S5 ≥ S3 > S2 > S1 > AS (Figure 7B) (female); interspinal space between S4 and S3 wide (male) or narrow (female); prolateral surface with enlarged spiniform tubercles with a reddish, ventrobasal macrosetae; proventral margin with two long spiniform tubercles (female) or blunt short tubercles (males).

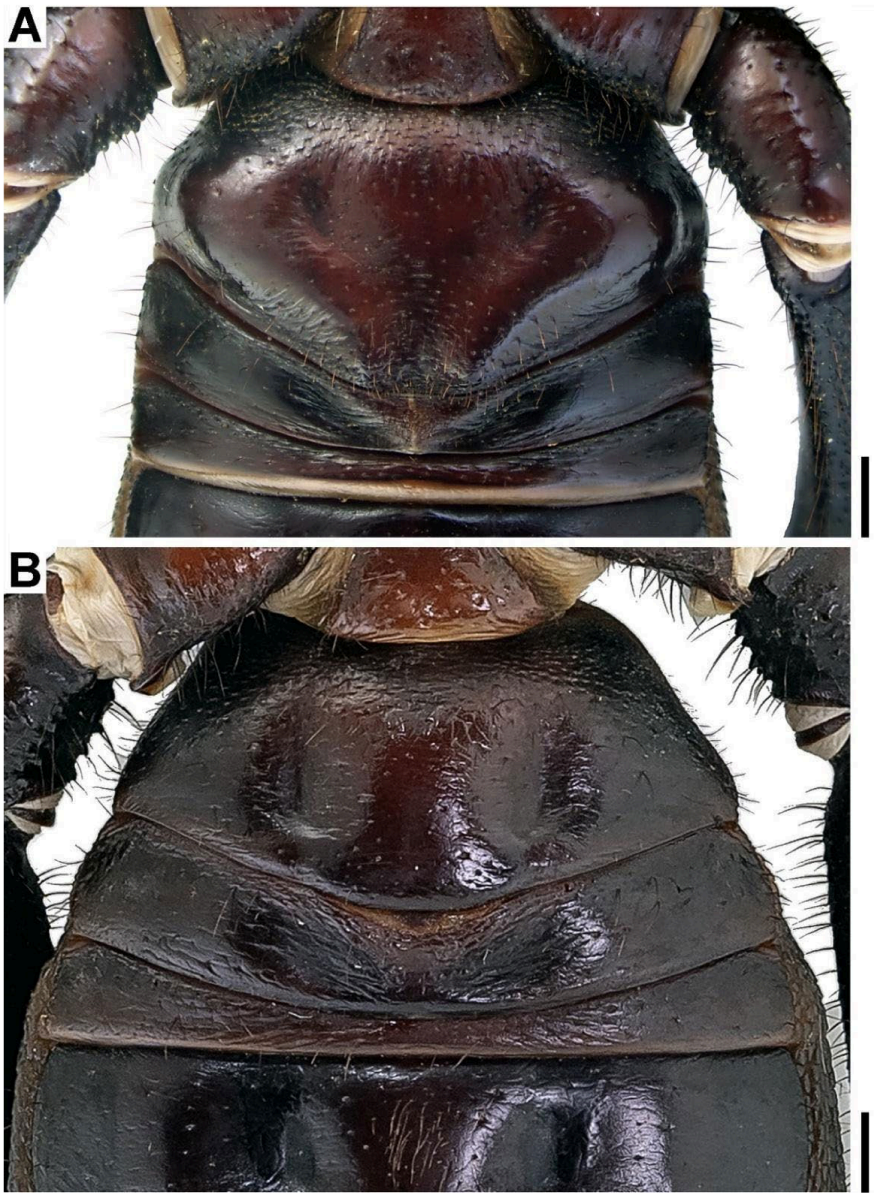

Figure 13. *Mastigoproctus claritae* sp. nov. Sternite II. Ventral view. Holotype ♂(CNAN-T1880) (**A**), Paratype ♀(CNAN-T1884) (**B**). Scale bar = 2 mm.

Femur dorsal surface reduced by compression of pro- and retrolateral surfaces (male) or without compression (female) (Figure 5C,D); prolateral surface with two spines, one prodorsal, short, sharply pointed and one proventral larger, blunt (male) (Figure 8A) or sharply pointed (female) (Figure 8B); retrolateral surface with congregated and blunt cristulae (male) (Figure 9) or reduced (female).

Patella slightly longer (male) or shorter (female) than tibia (Figure 5A,C, Table 1); prolateral surface with several reddish macrosetae; proventral margin with a subdistal

spine. Patellar apophysis elongated, almost one-quarter carapace length, granulated and slender (male) or shorter and robust (female) (Figure 5); base of patellar apophysis with two vestigial (male) or distinct (female) spines; prolateral and retrolateral margins with rows of serrated denticles; smaller and with less denticles (male), reddish macrosetae on all surfaces except prolateral. Tibia dorsal surface reduced by the compression of pro- and retrolateral surfaces (Figure 5A,C); prodorsal surface with a row of sparse, serrated denticles; proventral distal margin with two spines, proximal larger than distal. Fixed finger falciform, setose with an apical sharp claw, prolateral margin with a row of blunt, abundant denticles, retrolateral margin with row of sparse serrated denticles (Figure 10). Tarsus (movable finger), lateral margins with serrate row of denticles; retrolateral margin with a broad longitudinal rib and dorsal surface with a parallel rib (female) (Figure 10B), prolateral surface with a less developed rib or all ribs reduced (male) (Figure 10A); apex with a long claw (female) or shorter (male); all surfaces covered with reddish macrosetae, except apical claw.

Legs: Femur I surface with cristulae weakly developed and subapical setae, proventral surface on II–IV with cristulae, weakening distally, retroventral surfaces with vestigial cristulae and subapical macroseta. Patella I–IV mostly smooth surfaces with sparse setae. Tibiae I–IV smooth surfaces, on II–IV with a ventrodistal, spiniform, blackish spur; tibia I with one dorsal (Figure 11D) and one retrolateral trichobothria distally. Tarsus I with eight tarsomeres (±2) covered with orangish microsetae decreasing in size distally (Figure 11D), tarsus with tarsomeres gradually decreasing in length, with tarsomere I longest, except for the eighth tarsomere three fifths the length of first tarsomere. Basitarsi and telotarsi II–IV dorsal surfaces distal end with a paired blunt apophysis; ventral surfaces with a paired row of spiniform setae and apically flanked by larger, paired spur-like spines; telotarsi II–IV trisegmented with segments length: I (basal) > III (distal) > II (medial), covered with long, tapered setae of different size; telotarsi III armed with three dark brownish claws terminally, a pair of long falciform claws and a median short claw ventrodistally (Figure 11A–C).

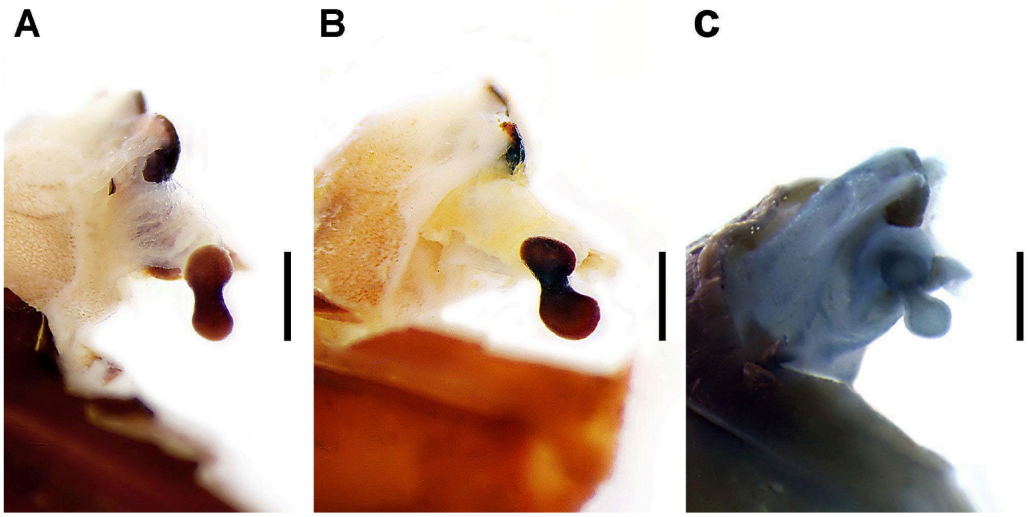

Figure 14. *Mastigoproctus* spermatecae. Lateral view. *Mastigoproctus claritae* sp. nov. Paratype ♀(CNAN-T1884) (**A**). *Mastigoproctus xetame* Paratype ♀(CNAN-T1504) (**B**), *Mastigoproctus mexicanus* ♀(CNAN-Ur0014) (**C**). Scale bar = 1 mm.

Opisthosoma: Tergites surface granular, more so on posterior margin, with microsetae throughout; tergite I–III with a median longitudinal suture evident; tergites IV–IX without suture, smooth. Tergite X (first segment of pygidium) with distinct lateral longitudinal sutures (pleuron), posterior margin with a granular row restricted to a dorsal semicircle.

Tergite XI smooth without suture, with posterior margin granular as tergite X. Tergite XII with a pair of posterolateral, ovate ommatoids (Figure 12).

Sternite II covering genital aperture, with a pair of submedian V-shaped (male) (Figures 1B and 13A) or lanceolate (female) depressions; posterolateral surfaces concave (male) or flat (female) (Figures 1C and 13B); posterior margin protruding markedly (male) or slightly (female), forming a median lobe, emarginated medially and overlapping with a sclerotized area in the space between sternites II and III (female). Sternite III divided longitudinally by a suture (male) or undivided (female) (Figure 13), with a pronounced anteriorly emargination, posterior margin with (male) or without (female) median patch of reddish macrosetae. Sternite IV undivided longitudinally. Sternite V with (male) or without (female) patch of fine golden macrosetae medially. Sternite VI–VIII surfaces smooth, with sparse fine, golden macrosetae. Sternite IX surface smooth with more abundant reddish macrosetae.

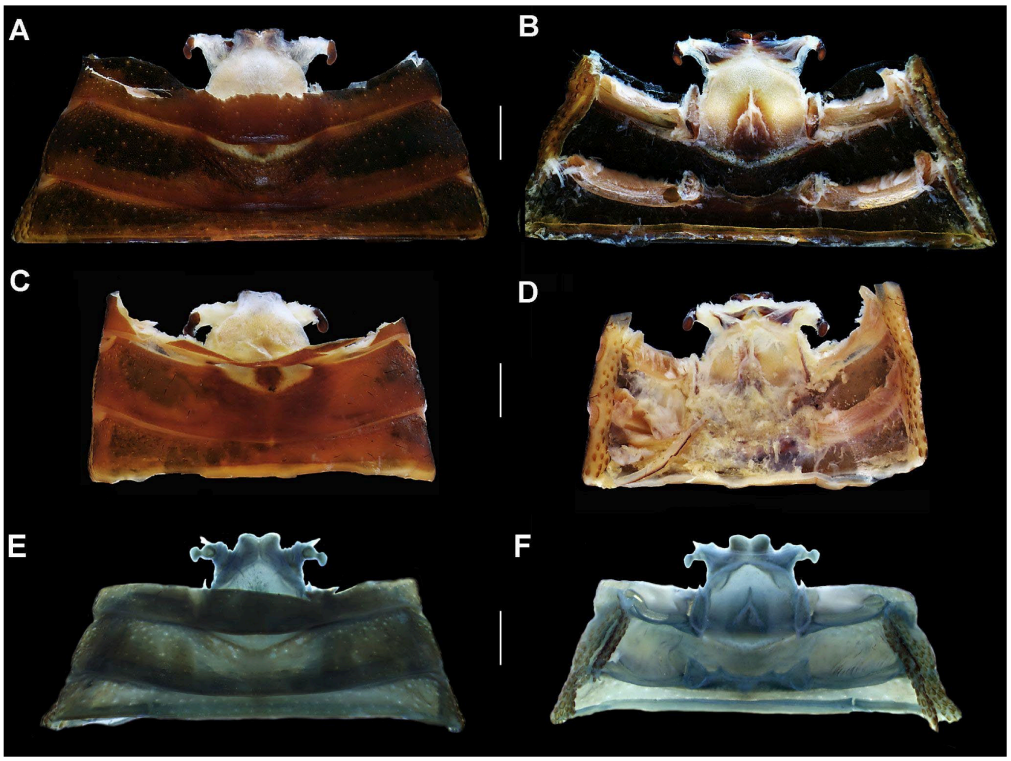

Figure 15. *Mastigoproctus* female genitalia. Dorsal (**B**,**D**,**F**) and ventral (**A**,**C**,**E**) view. *Mastigoproctus claritae* sp. nov. Paratype ♀(CNAN-T1884) (**A**,**B**). *Mastigoproctus xetame* Paratype ♀(CNAN-T1504) (**C**,**D**), *Mastigoproctus mexicanus* ♀(CNAN-Ur0014) (**E**,**F**). Scale bar = 2 mm.

Female genitalia: Spermatheca seminal receptacles peanut-shaped, symmetric, rounded, apex pointing posterodorsally (Figure 14A); spermathecal neck short, wide; aperture of uterus curved, with medial notch; atrium pentagonal in dorsal aspect (Figure 15A,B).

Male genitalia: Lobe lateralis primus physema-shaped, rounded longer than wider, bilobed proximally, with thin longitudinal wrinkles (Figure 16B,C). Lobe lateralis secundus globose, soft, mostly covered by the lobe lateralis primus (Figure 16C). Fistula with inverted triangular-shaped, strongly sclerotized, with rounded edges and anterior margin deep (Figure 16B,C). Lobe dorsal longer than wider, rimmed by a sclerotized margin. Lamina medialis covered by the lobe lateralis primus. Processus internus covered by the lamina medialis. Mensa subtriangular, smooth. Fulcrum minute (Figure 16C).

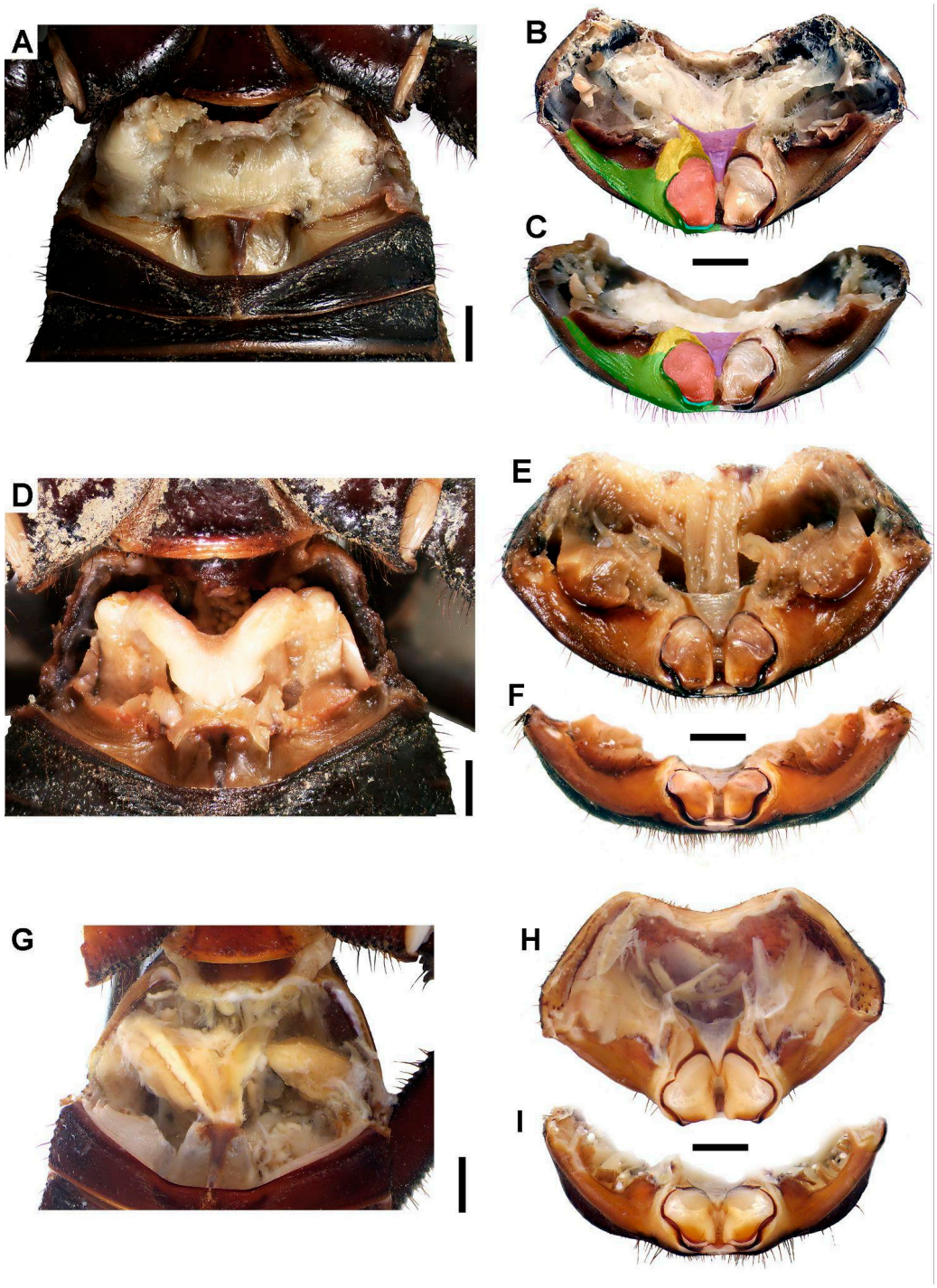

Figure 16. *Mastigoproctus* male genitalia. Dorsal (**B**,**E**,**H**), ventral (**A**,**D**,**G**) and posterior (**C**,**F**,**I**) view. *Mastigoproctus claritae* sp. nov. Paratype ♂(CNAN-T1882) (**A**,**B**,**C**), *Mastigoproctus xetame* ♂(CNAN-Ur0126) (**D**,**E**,**F**), *Mastigoproctus mexicanus* ♂(CNAN-Ur0058) (**G**,**H**,**I**). Green = **fistula**, yellow = **lobus dorsalis**, red = **lobus lateralis primus**, blue = **lobus lateralis secundus**, purple = **mensa**. Scale bar 2 = mm.

Flagellum: Flagellomeres cylindric, with scattered setae (Figure 17) arranged homogeneously in all surfaces. Flagellar organs elliptical or nearly so, situated near the anterior margin ventrally from second flagellomere onwards (Figure 17).

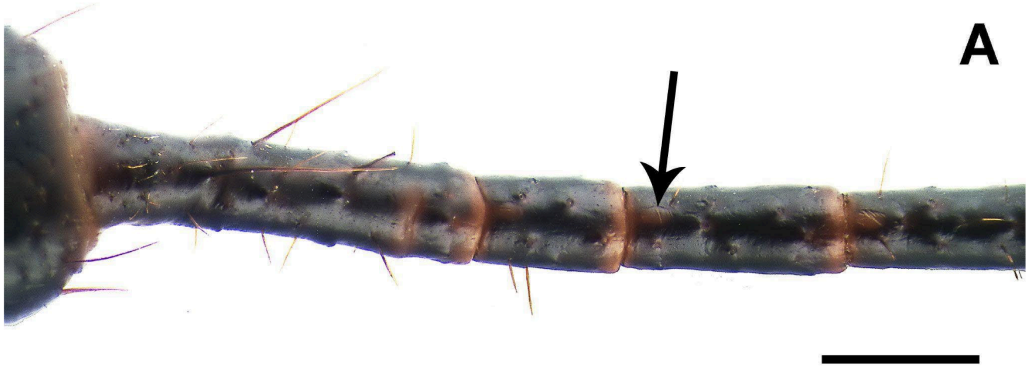

Figure 17. *Mastigoproctus claritae* sp. nov. Flagellum, lateral view. Holotype male (CNAN-T1880) (**A**). Arrow indicates flagellar organs. Scale bar = 2 mm.

Sexual dimorphism: Adult males present characters that differ from the females and immature stages. In immatures, the genitalia are not developed; therefore, sternite II is not modified (V-shaped or lanceolate depressions submedially, concave or flattened ventral surfaces) (Figure 13). Males are usually bigger than females in size (Figure 1). The pedipalps segments in males are longer than in females, and in females, the pedipalps segments are more robust (Figure 5). In females, all spines along the prodorsal margin of the pedipalp trochanter are evenly spaced, whereas a wider gap is present between spines S3 and S4 than between other spines in males; S4 is the longest in females, whereas in males, S3 is the longest, and there is an accessory spine present in females but absent in males (Figure 7). The retroventral spine on the pedipalp femur and the proventral spiniform tubercles on the trochanter are short and blunt in males, whereas in females, they are longer and sharply pointed (Figure 8). The patellar apophysis is slender and elongated in males, whereas it is short and robust with serrated denticles on lateral margins in females (Figure 5A,C). The movable finger in females has two well-developed longitudinal ribs in the retrolateral and dorsal surface, whereas in males, the ribs are reduced (Figure 10). The movable finger's claw is longer in females than in males. The posterolateral surfaces of sternite II are slightly incressate in males but flat in females. Two patches of macrosetae are present on ventral surfaces of sternites III and V in males, whereas they are absent in females.

Distribution. *Mastigoproctus claritae* sp. nov. has been reported [21] at the Estación de Biología Chamela, which lies within the Chamela-Cuixmala Biosphere Reserve in Jalisco, Mexico.

Natural history. During several expeditions to the Estación de Biología Chamela, where we were conducting fieldwork for our project on faunistic analyses of the order arachnid orders Scorpiones, Opiliones, and Pseudoscorpiones, we fortuitously encountered vinegaroon specimens of the species described here. We observed that *Mastigoproctus claritae* sp. nov. inhabits seasonal dry forest with a marked seasonality, at elevations ranging from 1 to 91 m, with a temperature range of 22.1–30.3 °C and a precipitation range from 780 to 1390 mm. During the dry season (Figure 18B), the presence of *Mastigoproctus claritae* sp. nov. becomes increasingly rare. Following the rainy season (Figure 18A), there is an increase in superficial activity, particularly among the males. This species appears to construct burrows during the dry season. Although we were unable to localize burrows in the field, we kept one specimen alive that burrowed in laboratory conditions. During periods of superficial activity coinciding with the rainy season, observations have been made of the species either walking on the surface of leaf litter or beneath rotten logs. However, it was observed that this species of vinegaroon also exhibited climbing behavior on tree trunks (Figure 19).

Table 1. Measurements (mm) of the type-series of *Mastigoproctus claritae* sp. nov.

Individual	Holotype ♂	Paratype ♂	Paratype ♂	Paratype ♂	Paratype ♀	Paratype ♀
Collection Code	**CNAN-T1880**	**CNAN-T1881**	**CNAN-T1882**	**CNAN-T1883**	**CNAN-T1884**	**CNAN-T1885**
Total length	57.2	57.3	56.1	70.8	56.6	58.1
Carapace						
Total length	20.76	20.44	20.52	26.64	20.26	21.13
Total width at median ocular tubercle	4.33	4.20	4.20	4.82	4.09	4.34
Total width at posterior fovea	11.26	11.26	12.20	16	11.69	11.30
Distance med. ocular tubercle to anterior margin	1.45	1.53	1.69	1.71	1.56	1.55
Median ocelli width	0.42	0.33	0.43	0.42	0.41	0.47
Total width at lateral ocelli	9.57	9.59	10.07	12.76	9.80	10.13
Distance between median ocelli	0.83	1	0.80	0.93	0.88	0.86
Pedipalp						
Coxa length	11.02	11.19	10.62	12.58	8.94	9.31
Coxa maximum width	6.58	6.94	6.90	9.19	6.68	7.08
Trochanter length	6.80	7.8	7.06	9.86	6.43	6.44
Trochanter width	5.61	5.72	5.66	7.57	5.63	5.92
Length S3 trochanter	1.03	1.07	1	1.25	-	-
Length S4 trochanter	0.79	0.76	0.79	1.24	-	-
Space length between S3 and S4	0.69	0.70	0.81	1.20	-	-
Femur length	12.31	14.05	13.28	20.90	9.68	10.02
Femur width	4.79	4.52	4.61	6.74	4.70	4.98
Ventromesal spine length	0.91	0.70	0.70	1.26	0.91	0.94
Ventromesal spine width	0.48	0.50	0.48	0.67	0.54	0.51
Patella length	9.32	9.47	10.31	15.12	7.15	7.99
Patella width	5.50	4.81	5.26	7.14	4.57	5.33
Patellar apophysis length	4.29	4.70	4.60	6.13	3.43	3.40
Patellar apophysis width	1.42	1.51	1.40	2.39	1.75	1.77
Tibia length	9.09	9.22	9.01	13.68	5.25	5.65
Tibia width	4.57	4.11	4.62	5.77	3.56	4.13
Tibial apophysis length	3.01	2.93	3.34	4.24	2.46	2.26
Tibial apophysis width	1.98	2	2.16	2.99	1.46	1.51
Tarsus length	6.30	6.54	6.84	8.63	6.21	5.32
Tarsus width	2.73	3.07	2.95	4.20	2.26	2.54
Leg I						
Coxa length	3.78	3.69	3.53	4.48	3.66	4.08
Trochanter length	3.65	3.37	3.71	4.99	3.43	3.51
Femur length	13.91	13.63	14.32	17.79	12.11	13.46
Patella length	18.83	18.03	19.48	23.68	16.43	17.72
Tibia length	19.23	18.66	18.83	23.63	16.79	17.77
Tarsus length	14.58	10.19	14.66	16.76	12.79	13.24
Leg IV						
Coxa length	6.48	6.74	6.46	8.38	6.39	6.94
Trochanter length	7.44	7.38	7.51	9.24	6.68	7.69
Femur length	16.26	16.50	16.60	20.50	15.26	15.84
Patella length	6.34	6.36	6.37	7.98	6.36	6.76
Tibia length	15.97	16.45	16.28	19.92	15.05	14.94
Basitarsus length	3.22	3.35	3.54	3.82	3.39	3.11
Telotarsus III length	1.77	1.80	1.84	2.16	1.85	1.82
Pygidium						

Table 1. *Cont.*

Individual	Holotype ♂	Paratype ♂	Paratype ♂	Paratype ♂	Paratype ♀	Paratype ♀
Collection Code	**CNAN-T1880**	**CNAN-T1881**	**CNAN-T1882**	**CNAN-T1883**	**CNAN-T1884**	**CNAN-T1885**
Ommatoid height	0.28	0.31	0.33	0.43	0.28	0.37
Ommatoid width	0.15	0.21	0.22	0.25	0.20	0.22
Ommatoid height:pygidium height	0.08	0.10	0.10	0.11	0.08	0.11
Male genitalia						
Lobus lateralis primus width: sternite II width	-	0.17	0.19	0.16	-	-

Table 2. Mexican species of the thelyphonid genus *Mastigoproctus* Pocock, 1894.

Species	Distribution
Mastigoproctus cinteotl Barrales-Alcalá, Francke & Prendini, 2018	Querétaro, San Luis Potosí, Tamaulipas
Mastigoproctus claritae sp. nov.	Jalisco
Mastigoproctus franckei Barrales-Alcalá, 2025	San Luis Potosí
Mastigoproctus giganteus (Lucas, 1835)	Morelos
Mastigoproctus lacandonensis Ballesteros & Francke, 2006	Chiapas
Mastigoproctus mexicanus (Butler, 1872)	Aguascalientes, Durango, Jalisco, Zacatecas
Mastigoproctus scabrosus (Pocock, 1902)	Oaxaca, Veracruz
Mastigoproctus spinifemoratus Castro-Pereira, Pinto-da-Rocha & Prendini 2025	Nuevo León, Tamaulipas
Mastigoproctus tohono Barrales-Alcalá, Francke & Prendini, 2018	Aguascalientes, Arizona, Sonora
Mastigoproctus vandevenderi Barrales-Alcalá, Francke & Prendini, 2018	Sonora
Mastigoproctus xetame Barrales-Alcalá & Francke, 2025	Jalisco
Mastigoproctus yalchanchak Barrales-Alcalá & Francke 2025	Chiapas

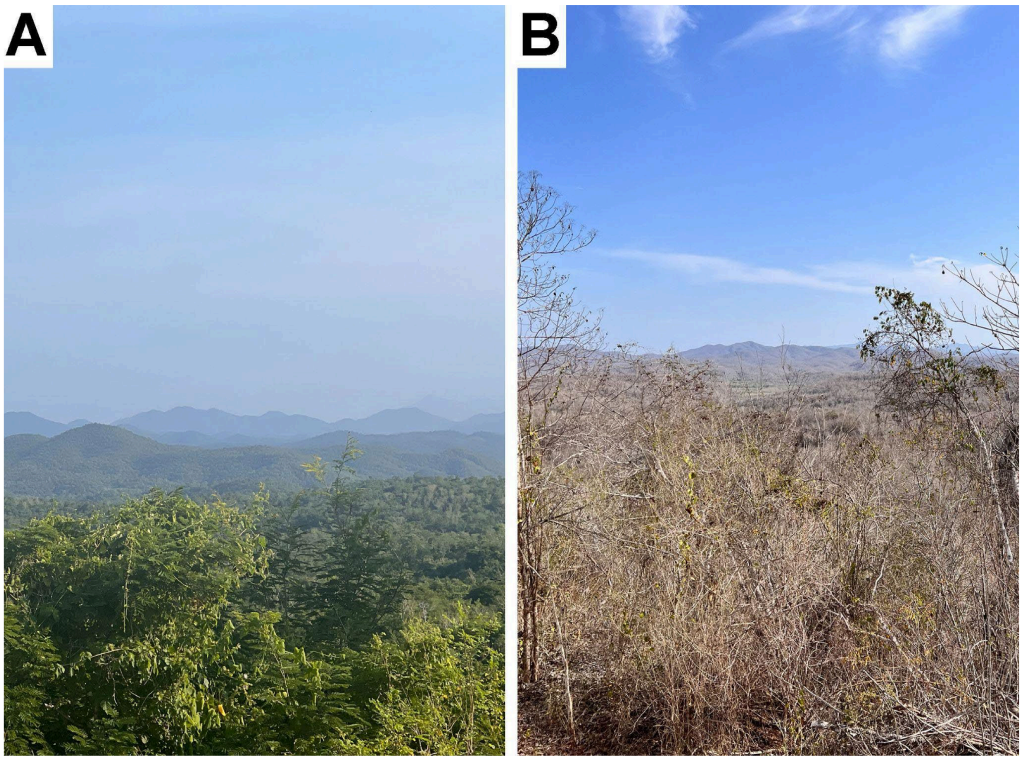

Figure 18. Chamela-Cuixmala Biosphere Reserve during the rainy season (**A**) and dry season (**B**).



Figure 19. *Mastigoproctus claritae* sp. nov. male and female specimens climbing tree trunks at the Chamela-Cuixmala Biosphere Reserve, Jalisco.

4. Discussion

As demonstrated in [22], Mexico has been shown to exhibit a higher level of biodiversity than other regions of the world with respect to the arachnid orders Ricinulei Thorell, 1876; Palpigradi Thorell, 1888; Scorpiones C. L. Koch, 1850; and Pseudoscorpiones de Geer, 1778. In contrast, vinegaroons represent a less diverse arachnid order. Nevertheless, *Mastigoproctus* is the second-most speciose vinegaroon genus worldwide [14].

The World Uropygi Catalog [14] lists 22 extant valid species within the genus *Mastigoproctus*. However, in 2023, three species were described: *Mastigoproctus franckei* Barrales-Alcalá, 2023; *Mastigoproctus xetame* Barrales-Alcalá & Francke, 2023; and *Mastigoproctus yalchanchak* Barrales-Alcalá & Francke 2023 [16]. These were all found in Mexico. Additionally, *Mastigoproctus spinifemoratus* Castro-Pereira, Pinto-da-Rocha & Prendini 2025, from the same country, was described [17], bringing the total to 26 species. However, Ref. [19] transferred *Mastigoproctus annectens* Werner, 1916; *Mastigoproctus butleri* Pocock, 1894; and *Mastigoproctus perditus* Mello-Leitão, 1931, to the genus *Amauromastigon* Mello-Leitão, 1931, and *Mastigoprotus minensis* Mello-Leitão, 1931, to the genus *Heptatarsus* Castro-Pereira & Pinto-da-Rocha, 2025, on the basis of molecular analysis. Therefore, the total number of *Mastigoproctus* species in the Americas, including *Mastigoproctus claritae* sp. nov., currently comprises 23, with 12 of them being distributed in Mexico (Table 2, Figure 20).

The intricate geological history, marked by phenomena such as mountain uplifts, volcanic activity, and fluctuations in sea level, may have exerted a profound influence on this elevated biodiversity [22,23]. A significant factor that may contribute to the proliferation of new species is the availability of a vast array of habitats. For instance, in Jalisco, the *Mastigoproctus* species *M. mexicanus* and *M. xetame* are present in the northern portion of the state, occupying mixed pine–oak forests at elevations ranging from 1400 to 2000 m [15,16]. Conversely, *Mastigoproctus claritae* sp. nov. was identified in seasonal dry forest at lower elevations (up to 100 m) within the coastal zone of Jalisco (Figure 20). This species distribution suggests a pattern of endemism, which is common in burrowing and poor-dispersing species [24–28] such as vinegaroons. A similar pattern has been observed in several Mexican scorpions, including the genus *Diplocentrus* in Oaxaca [29], as well as

in several vaejovids in the Baja California peninsula [30]. Further studies are necessary to fully understand the richness of *Mastigoproctus* in Mexico.

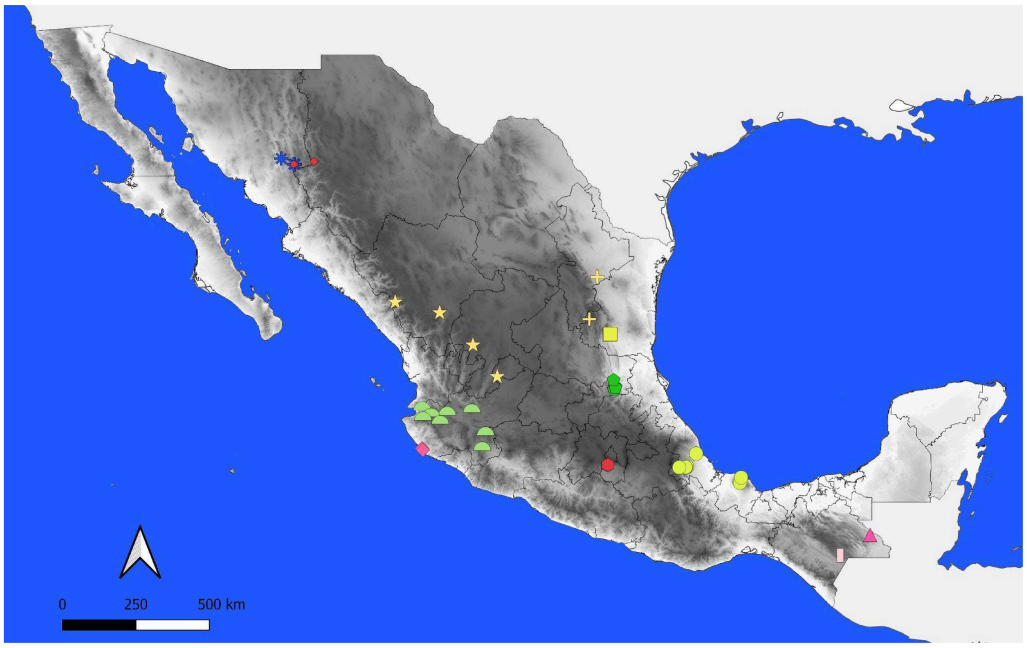

Figure 20. Map of Mexico with an updated distribution of Mexican species of the genus *Mastigoproctus* Pocock, 1894. *Mastigoproctus cinteotl* Barrales-Alcalá, Francke & Prendini, 2018 (**yellow square**). *Mastigoproctus claritae* sp. nov. (**pink diamonds**). *Mastigoproctus franckei* Barrales-Alcalá, 2025 (**green pentagons**). *Mastigoproctus giganteus* (Lucas, 1835) (**red hexagons**). *Mastigoproctus lacandonensis* Ballesteros & Francke, 2006 (**pink triangle**). *Mastigoproctus mexicanus* (Butler, 1872) (**yellow stars**). *Mastigoproctus scabrosus* (Pocock, 1902) (**yellow circles**). *Mastigoproctus spinifemoratus* Castro-Pereira, Pinto-da-Rocha & Prendini 2025 (**yellow crosses**). *Mastigoproctus tohono* Barrales-Alcalá, Francke & Prendini, 2018 (**blue asterics**). *Mastigoproctus vandevenderi* Barrales-Alcalá, Francke & Prendini, 2018 (**red circles**). *Mastigoproctus xetame* Barrales-Alcalá & Francke, 2025 (**green semicircles**). *Mastigoproctus yalchanchak* Barrales-Alcalá & Francke 2025 (**pink rectangle**). Localities taken from [14–17].

The natural history of vinegaroons is poorly understood due to their strictly nocturnal habits, cryptic coloration, slow movement, and scarce superficial activity. It has been documented that vinegaroons inhabiting deserts only emerge from their burrows after the first summer rain during brief periods [25]. However, the discovery of specimens of *Mastigoproctus claritae* sp. nov. climbing on three trunks is particularly intriguing and offers novel insights into their behavioral patterns (Figure 19). However, it is challenging to offer a compelling explanation of this behavior at this juncture. As [15] suggests, the delimitation of additional species will facilitate comparative studies on various aspects of their biology, habitats, and behavior.

The efficacy of employing standardized landmarks for species descriptions and morphological studies of various arachnid groups, including scorpions and spiders, has been demonstrated [31]. Standardized measurements for the vinegaroon have not yet been documented in the extant literature. Consequently, we advocate for the standardization of landmarks in forthcoming taxonomic and systematic studies.

Despite the advances of [15–17] in morphological traits used in *Mastigoproctus* descriptions, further exploration is necessary. For instance, the male genitalia of most *Mastigoproctus* species remain to be fully described [17]. A thorough review of the extant literature reveals that the male genitalia of some species of the following genera have been described: *Amauromastigon* Mello-Leitão, 1931; *Heptatarsus* Castro-Pereira & Pinto-da-Rocha [19]; *Typopeltis* Pocock, 1894 [20]; *Wounaan* Botero-Trujillo, Moreno-González & Prendini, 2024; and

Yekuana Botero-Trujillo, Moreno-González & Prendini, 2024 [32]. To date, the *Mastigoproctus* genus has been found to contain only one species for which a male genitalia description has been recorded: *M. spinifemoratus* [17]. In this study, we present photographic documentation of the male genitalia of three additional species: *Mastigoproctus claritae* sp. nov. (Figure 16A–C), *M. xetame* (Figure 16D–F), and *M. mexicanus* (Figure 16G–I). We have identified that the morphology of the lobus lateralis primus and the sclerotized margins of the lobus dorsalis and fistula exhibit potential taxonomic markers for distinguishing *Mastigoproctus* species. In accordance with the proposal outlined by [19,20,32], we have undertaken a comprehensive description of the genitalia for the species *M. xetame* and *M. mexicanus*, which, in terms of both morphological characteristics and geographical distribution, exhibits similarity to *Mastigoproctus claritae* sp. nov. Our comparative studies, which examined diverse perspectives on the structures, yielded novel characters that exhibited sufficient variation to be proposed as diagnostic characters. For instance, in the newly described species *Mastigoproctus claritae* sp. nov., the median ocular tubercle is conspicuously protruding from the carapace, and the eye socket is wider. In contrast, in *M. xetame*, the tubercle is located lower on the carapace, and the eye socket is smaller (Figure 3C,D), whereas *M. mexicanus* exhibits an intermediate protrusion (Figure 3E,F). A secondary character system that was rediscovered pertains to the ornamentation of the pedipalp surfaces, a common feature in the classification of species within the *Mastigoproctus giganteus* complex [15] (Figure 9). The cristulae in male *Mastigoproctus claritae* sp. nov. specimens are congregated and blunt; in *M. xetame*, they are scattered and conical; and in *M. mexicanus*, they are straight and digitiform tubercles. This character system may contain valuable information for distinguishing other species and requires further exploration. The spermathecae of *Mastigoproctus claritae* sp. nov. exhibit a symmetrical morphology (Figures 14A and 15A,B), while those of *M. xetame* display an asymmetrical medial axis (Figures 14B and 15C,D), and those of *M. mexicanus* are obovate (Figures 14C and 15E,F). In future taxonomic studies, we advocate for the incorporation of female and male genitalia, as they contain diagnostic characters. In summary, further exploration of classical morphology is warranted as is an integrative vision for delimiting extant species awaiting taxonomic studies.

Author Contributions: Conceptualization, E.G.-S., A.F.A.L., and C.A.T.-M.; methodology, C.A.T.-M. and E.G.-S.; investigation, E.G.-S. and C.A.T.-M.; resources, E.G.-S. and A.F.A.L.; data curation, E.G.-S. and C.A.T.-M.; writing, C.A.T.-M., E.G.-S., and A.F.A.L.; original draft preparation, C.A.T.-M., E.G.-S., and A.F.A.L.; writing—review and editing, C.A.T.-M., E.G.-S., and A.F.A.L. All authors have read and agreed to the published version of the manuscript.

Funding: This research received no external funding.

Institutional Review Board Statement: This study was guided by the General Wildlife Law, its Regulations, or the revised Mexican Official Standards (NOMs), none of which mandate formal ethics committee approval for wild animal euthanasia conducted solely for taxonomic curation. To further ensure ethical compliance, we consulted our local committee (CoÉTICA-IBUNAM) on this issue, and they determined that the article submitted for evaluation meets the basic criteria of bioethics and research ethics according to the current guidelines of UNAM and the recommendations of other national and international bodies.

Data Availability Statement: The original contributions presented in this study are included in the article. Further inquiries can be directed to the corresponding author.

Acknowledgments: We would like to express our gratitude to Dirección General de Asuntos del Personal Académico (DGAPA) from the Universidad Nacional Autónoma de México for a postdoctoral fellowship to A.F.A.L. We are also grateful to Katherine Renton, Enrique Ramírez García, and Sayra Siordia from Estación de Biología Chamela for their invaluable assistance during the fieldwork. We

would also like to express our gratitude to Daniel Ochoa Vázquez for his assistance in photography and to Fernando Álvarez Padilla and Griselda Montiel Parra for their contribution of specimens for this study. We would like to express our gratitude to Academic Editor Matthew Graham and the four anonymous reviewers for their constructive feedback, which significantly enhanced the quality of the manuscript.

Conflicts of Interest: The authors declare no conflicts of interest.

References

1. Pim, S.L.; Russel, G.J.; Gittleman, J.L.; Brooks, T.M. The future of biodiversity. *Science* **1995**, *269*, 347–350. [CrossRef]
2. Singh, J.S. The biodiversity crisis: A multifaceted review. *Curr. Sci.* **2002**, *82*, 638–647.
3. Shivanna, K.R. The sixth mass extinction crisis and its impact on biodiversity and human welfare. *Resonance* **2020**, *25*, 93–109. [CrossRef]
4. Kim, K.C.; Byrne, L.B. Biodiversity loss and the taxonomic bottleneck: Emerging biodiversity science. *Ecol. Res.* **2006**, *21*, 794–810. [CrossRef]
5. Hortal, J.; De Bello, F.; Diniz-Filho, J.A.F.; Lewinsohn, T.M.; Lobo, J.M.; Ladle, R.J. Seven shortfalls that beset large-scale knowledge of biodiversity. *Ann. Rev. Ecol. Evol. Syst.* **2015**, *46*, 523–549. [CrossRef]
6. Cornwell, W.K.; Pearse, W.D.; Dalrymple, R.L.; Zanne, A.E. What we (don't) know about global plant diversity. *Ecography* **2019**, *42*, 1819–1831. [CrossRef]
7. Lessa, T.; Stropp, J.; Hortal, J.; Ladle, R.J. How taxonomic change influences forecasts of the Linnean shortfall (and what we can do about it)? *J. Biogeogr.* **2024**, *51*, 1365–1373. [CrossRef]
8. Harvey, M.S. The neglected arachnids: What do we know about the smaller arachnid orders? *J. Arachnol.* **2002**, *30*, 357–372. [CrossRef]
9. Harvey, M.S. The smaller arachnid orders: Diversity, descriptions and distributions from Linnaeus to the present (1758 to 2007). *Zootaxa* **2007**, *1668*, 363–380. [CrossRef]
10. Zhang, Z.-Q. Phylum Arthropoda von Siebold, 1848. In Animal biodiversity: An outline of higher-level classification and survey of taxonomic richness (pp. 17–55). *Zootaxa* **2013**, *3703*, 1–82. [PubMed]
11. World Spider Catalog 2026. World Spider Catalog. Version 27. Natural History Museum Bern. Available online: http://wsc.nmbe.ch (accessed on 9 June 2026).
12. Schmidt, J.O.; Schmidt, L.S. Vinegaroons (Uropygi: *Mastigoproctus tohono*) in a multi-predator/multi-prey system: Prey, predators, and cannibalism. *J. Arachnol.* **2022**, *50*, 267–276. [CrossRef]
13. Agnarsson, I. Grand challenges in research on arachnid diversity, conservation, and biogeography. *Front. Arachn. Sci.* **2023**, *2*, 1101141. [CrossRef]
14. World Uropygi Catalog. Natural History Museum Bern. 2025. Available online: http://wac.nmbe.ch (accessed on 3 March 2025).
15. Barrales-Alcalá, D.A.; Francke, O.F.; Prendini, L. Systematic revision of the giant vinegaroons of the *Mastigoproctus giganteus* complex (Thelyphonida: Thelyphonidae) of North America. *Bull. Am. Mus. Nat. Hist.* **2018**, *418*, 1–62. [CrossRef]
16. Barrales-Alcalá, D.A.; Francke, O.F. Three new species of the giant vinegaroon genus *Mastigoproctus* (Thelyphonida: Thelyphonidae) from Mexico. *J. Arachnol.* **2023**, *51*, 223–237. [CrossRef]
17. Castro-Pereira, D.; Pinto-da-Rocha, R.; Prendini, L. *Mastigoproctus spinifemoratus*, a new species of giant vinegaroon (Thelyphonida: Thelyphonidae) from Mexico. *Arthropoda* **2025**, *3*, 2. [CrossRef]
18. Snodgrass, R.E. The feeding organs of Arachnida, including mites and ticks. *Smithson. Misc. Collect.* **1948**, *110*, 26–31.
19. Castro-Pereira, D.; Pinto-da-Rocha, R. Molecular phylogeny and systematic revision of the Brazilian species of *Mastigoproctus* Pocock, 1894 (Arachnida: Uropygi: Mastigoproctinae). *Invertebr. Syst.* **2025**, *39*, IS24068. [CrossRef]
20. Seraphim, G.; Giupponi, A.P.L.; Miranda, G.S. Taxonomy of the thelyphonid genus *Typopeltis* Pocock, 1894, including homology proposals for the male gonopod structures. *ZooKeys* **2019**, *848*, 21–39. [CrossRef]
21. Lira, A.F.A.; del-Pozo, O.G.; Contreras-Félix, G.A. Report of giant vinegaroon (Thelyphonida: Thelyphonidae) predation by scorpion (Scorpiones: Buthidae) in Mexican tropical dry forest. *Acta Arachnol.* **2025**, *74*, 27–29. [CrossRef]
22. Ponce-Saavedra, J.; Jiménez, M.L.; Quijano-Ravell, A.F.; Vargas-Sandoval, M.; Chamé-Vázquez, D.; Palacios-Cardiel, C.; Maldonado-Carrizales, J. The Fauna of Arachnids in the Anthropocene of Mexico. In *Mexican Fauna in the Anthropocene*, 1st ed.; Jones, R.W., Patricia Ornelas-García, C., Pineda-López, R., Álvarez, F., Eds.; Springer: Cham, Switzerland, 2023.
23. Ramamoorthy, T.P.; Bye, R.; Lot, A.; Fa, J. *Biological diversity of Mexico: Origins and Distribution*; Oxford University Press: New York, NY, USA, 1993.
24. Koleff, P.; Urquiza-Haas, T.; Ruiz-González, S.P.; Hernández-Robles, D.R.; Mastretta-Yanes, A.; Quintero, E.; Sarukhán, J. Biodiversity in Mexico: State of Knowledge. In *Global Biodiversity: Volume 4: Selected Countries in the Americas and Australia*, 1st ed.; Pullaiah, T., Ed.; Apple Academic Press: Palm Bay, FL, USA, 2018.

25. Schmidt, J.O.; Schmidt, L.S. Natural history, phenology, population density, and injuries/regeneration of the vinegaroon (Uropygi: Thelyphonidae: *Mastigoproctus tohono*). *J. Arachnol.* **2025**, *52*, 214–221. [CrossRef]
26. Hamilton, C.A.; Hendrixson, B.E.; Bond, J.E. Taxonomic revision of the tarantula genus *Aphonopelma* Pocock, 1901 (Araneae, Mygalomorphae, Theraphosidae) within the United States. *ZooKeys* **2016**, *560*, 1–340. [CrossRef] [PubMed]
27. Prendini, L. Substratum specialization and speciation in southern African scorpions: The Effect Hypothesis revisited. In *Scorpions 2001. Memoriam Gary A. Polis*; Fet, V., Selden, P.A., Eds.; British Arachnological Society, Burnham Beeches: Buckinghamshire, UK, 2001; pp. 113–139.
28. González-Santillán, E. Diversidad, taxonomía y hábitat de alacranes. In *Artrópodos de Chamela*; García, A.N., Ayala, R., Eds.; Instituto de Biología, UNAM: Ciudad de México, Mexico, 2004; pp. 25–35.
29. Francke, O.F. Scorpions of the genus *Diplocentrus* from Oaxaca, Mexico. *J. Arachnol.* **1977**, *4*, 145–200.
30. Williams, S.C. Scorpions of Baja California, Mexico and adjacent islands. *Occas. Pap. Calif. Acad. Sci.* **1980**, *135*, 1–127.
31. Polis, G.A. Field and Laboratory Methods. In *The Biology of Scorpions*; Polis, G.A., Ed.; Stanford University Press: Stanford, CA, USA, 1990; pp. 215–221.
32. Botero-Trujillo, R.; Moreno-González, J.A.; Prendini, L. Phylogeny of the neotropical hypoctonine whip-scorpions (Thelyphonida, Thelyphonidae), with descriptions of two new genera and species. *Insects* **2024**, *15*, 761. [CrossRef]

Disclaimer/Publisher's Note: The statements, opinions and data contained in all publications are solely those of the individual author(s) and contributor(s) and not of MDPI and/or the editor(s). MDPI and/or the editor(s) disclaim responsibility for any injury to people or property resulting from any ideas, methods, instructions or products referred to in the content.